Dynamics of Defect Annihilations in Polymerization of Aromatic Liquid Crystalline Polyesters

Yan Wang,[†,‡] Tai-Shung Chung,[*,§] Si-Xue Cheng,[||] and Jingmei Xu[‡]

Department of Chemistry, National University of Singapore, 10 Kent Ridge Crescent, Singapore 119260, Institute of Materials Research and Engineering, 3 Research Link, Singapore 117602, Department of Chemical and Environmental Engineering, National University of Singapore, 10 Kent Ridge Crescent, Singapore 119260, and Department of Chemistry, Wuhan University, Wuhan 430072, People's Republic of China

Received: May 5, 2003; In Final Form: August 11, 2003

We have studied the annihilation process of disclinations during in situ thin film polymerization of a series of aromatic liquid crystalline polyesters by using a polarizing light microscope (PLM). The decreases both in isotropic molten area during liquid crystal (LC) phase formation and in distance between LC disclination pairs during annihilation are found to follow a power law relation. However, abnormal annihilation phenomena, which have not been previously reported, are observed. A faster annihilation rate in the late stage of the annihilation process and an increase in the distance of a disclination pair can occur if the LC system is a reacting system or if the surroundings have other ongoing annihilations.

1. Introduction

It has been found that ordered systems quenched from a disordered state often evolve patterns of some characteristic sizes as they return to equilibrium. The complicated phenomena have been studied theoretically and numerically with the aid of computer simulations, which predict that the defect density and scale decay with time (t) following a $t^{-\nu}$ relationship where the exponent depends on details of the order parameter and the spatial dimensionality.[1−6]

Liquid crystals provide a valuable system to study the dynamics of topological defects. This is due to the fact that different kinds of stringlike (twist) or pointlike (wedge) defects can be created and controlled through symmetry-breaking phase transitions and the defects can be observed with optical microscopy. In addition, the experimental results obtained from the study of liquid crystals appear to be universal; thus, they can be further utilized for the study of similar situations in cosmology, particle physics, and condensed matter physics.

Studies on various liquid crystal (LC) defects have been conducted on LCs quenched from an isotropic to a nematic phase.[7−12] It has been reported that such defects also exist in the liquid crystal polymers (LCPs) solidified from their LC melts.[13−18] Earlier works have shown that the defect type and density strongly influence the rheological behavior and mechanical properties of LCPs.[19−22] Among various kinds of defects, line defects, also called disclinations, are particularly important. Generally, when an LC or LCP system is quenched from an isotropic to a nematic state, topological defects called disclinations are created spontaneously. These defects are unstable and evolve with time after the quench.

Defects in a two-dimensional ($d = 2$) view can be assigned a strength and a sign, and may be treated as a charge.[37] Defects with opposite signs attract each other with a force proportional to the inverse of separation distance between them and annihilate. Defects with the same signs repel and push one another toward oppositely signed defects for eventual annihilation. Consequently, the number of defects in the system decreases with time. In three dimensions ($d = 3$), the disclinations exist as lines or strings. During coarsening, the density of disclination decreases. The evolution process of defect annihilation with time occurs in both two and three dimensions via a highly cooperative pathway mediated by the anisotropic elastic medium.

The dynamics study of various LC systems indicates that the defect density $\rho(t)$ decreases with time t following a power law relationship during the quench from a disordered to an ordered state as follows:

$$\rho(t) \sim t^{-\nu} \tag{1}$$

where ν is the scaling exponent which is a constant for a certain annihilation system. In most cases, ν is less than 1. However, some theoretical analyses suggest that ν is dependent on the spatial dimensionality (d). For stringlike defects, $\nu = 1$ at $d = 3$ and $\nu = 0.5$ at $d = 2$, while for pointlike defects $\nu = 1$ at $d = 3$.[1,3,7,23] Experimental results obtained from low molecular weight (LMW) LCs with stringlike defects and pointlike defects, and from LCPs with pointlike defects, show agreement with the theoretical predications.[7,9−11,23−26] Nevertheless, different values of ν have also been reported in recent theoretical and numerical studies of defect dynamics.[6,17,27−35,36] For example, $\nu = 0.7$ was experimentally observed in the pointlike defects of LC polyester films laid on a glass plate with surfaces exposed to air.[13] Another expression for the defect density vs time relationship was also reported. For example, both experimental and theoretical results indicate that the coarsening process of LMW smectic C liquid crystals is given by $\rho(t) \sim e^{-at}$ rather than $\rho(t) \sim t^{-\nu}$.[36] This discrepancy implies that boundary conditions and inherent properties of LC substances play important roles on the coarsening dynamics.

The number of pointlike defects created in thin LCP films during a phase transition is much greater than that in LMW

* Address correspondence to this author. Fax: 65-6779-1936. E-mail: chencts@nus.edu.sg.
[†] Department of Chemistry, National University of Singapore.
[‡] Institute of Materials Research and Engineering.
[§] Department of Chemical and Environmental Engineering, National University of Singapore.
[||] Wuhan University.

10.1021/jp030570w CCC: $27.50
Published on Web 01/07/2004

LCs, implying that LCPs may provide a good model system for studying the dynamics of topological defects. Thus the primary objectives of our paper are to investigate the details of evolution of defect annihilation and the dynamics and mechanisms of reorganizations of disclinations during the thin film polymerization of various aromatic LC polyesters. The thin film polymerization technique is used in this study because it has been proven to be a powerful and simple technique to in situ investigate reaction systems of thermotropic LCPs.[38−39]

2. Experimental Section

Monomers used for the reaction systems in this study are *p*-acetoxybenzoic acid (ABA), 2,6-acetoxynaphthoic acid (ANA), 4,4′-biphenol (BP), diacetoxybiphenyl (DABP), acetoxyacetanilide (AAA), and 2,5-thiophenedicarboxylic acid (TDA). BP was purchased from Aldrich and used as received, ABA, ANA, AAA, and DABP were acetylated from *p*-HBA (Teijin, Japan), 2,6-hydroxynaphthoic (HNA), *p*-aminophenol, and BP, respectively, according to literature reports.[38−40] 2,5-Thiophenedicarboxylic acid (TDA) was synthesized according to ref 41. The success of acetylation and synthesis was confirmed by ^{1}H NMR spectra. The melting points of ABA, ANA, BP, DABP, AAA, and TDA are 196, 226, 282, 163, 157, and 333 °C respectively, as tested by DSC (Perkin-Elmer DSC Pyris 1).

The following series of reaction systems were employed to confirm the universality of the experimental results obtained in the LC reaction systems. They are ABA/BP/TDA, ABA/DABP/TDA, ABA/AAA/TDA, ANA/BP/TDA, ANA/DABP/TDA, and ANA/AAA/TDA at a 70/15/15 molar ratio.

To carry out thin film polymerization under a polarizing microscope, monomers with a certain molar ratio were mixed and ground into a fine powder. About 2 mg of the monomer mixture was placed on a glass slide, and then several drops of acetone was deposited on the glass slide to dissolve the monomers. After evaporation of the solvent, a thin layer of the reactant mixture was formed and attached to the glass slide and then sandwiched between two glass slides with a ring spacer. The ring spacer was made of stainless steel with a thickness of 0.5 mm. The ring spacer provided space for easy removal or release of acetic acid during polymerization. Without the spacer, it was found that the reproducibility was quite low and the film quality was poor because the evaporation (or release) of acetic acid at elevated temperatures was vigorous. The polymerization reaction was then carried out on the top slide, and the thickness of the suspended thin film was controlled at about 10 μm. The whole package was placed on a heating stage (Linkam THMS-600) of a microscope and heated to a proposed temperature, 380 °C, with a heating rate of 90 °C/min. The sample was held at 380 °C during the whole reaction process. When the heating stage reached the proposed temperature, the reaction time began to be recorded. The temperature of the top slide was calibrated by measuring the melting points of the pure monomers as well as by measuring with a thermocouple. The polymerization was carried out on the top slide, and all the temperatures mentioned refer to the temperature of the top slide. The reaction process was observed in situ by a polarized light microscope (PLM) (Olympus BX 50) with crossed polarizers, between which a red plate having the retardation of 530 nm was inserted or not inserted. The sample package for thin film reaction in our study is shown in Figure 1.

The PLM micrographs were analyzed by an imaging software (Image-Pro Plus 3.0), which automatically calculated the distance between two defective points of a nonlinear disclination pair once we selected them from the photo image. The calculation of areas was made through a similar method. The perimeter of a specified area was drawn by hand along the edge, and the software calculated the perimeter and the contained area.

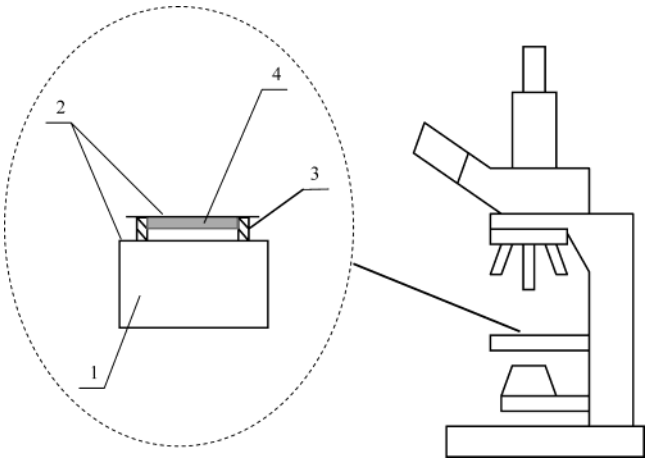

Figure 1. Sample package for thin film polymerization. 1, heating stage; 2, glass slides; 3, steel ring; 4, reaction system.

FTIR spectra of the monomer mixture before reaction and after thin film polymerization were recorded by a Perkin-Elmer (Beaconsfield, Bucks, UK) Spectrum 2000 FTIR spectrometer. The polymers obtained by thin film polymerization were scraped carefully from the glass slides without any further treatment and prepared as KBr pellets for IR measurements.

3. Results and Discussion

3.1. Morphological Changes of LC Textures during Thin Film Reaction. Polarized optical microscopy is one of the most popular tools to study liquid crystals. When all the directors are within the planes parallel to the glass slide on which a nematic liquid crystalline polymer is placed, a schlieren texture can be observed between crossed polarizers. The disclination lines can be clearly characterized by the analysis of the dark lines called "dark brushes" in the schlieren texture. The dark brushes correspond to the extinction positions, indicating that the directors are either parallel or normal to the electric vector of the polarizer or analyzer. The points at which the dark brushes meet indicate singular points and correspond to the disclination lines normal to the film surface.

In our systems, the molecular weight and chain length increase with reaction time. When the chain length of oligomers reaches a certain value, they form an anisotropic phase (LC phase) and separate from the isotropic melt. Because of the polydispersity, oligomers are partitioned within the isotropic and anisotropic phases according to their chain lengths. A fraction of oligomer molecules with relatively longer chain lengths forms anisotropic domains, while others remain in the isotropic phase. After the appearance of an anisotropic phase, the size of LC domains quickly increases, and correspondingly the number of domains decreases because of domain growth and coalescence of adjacent LC domains.

During the isothermal reaction, we can observe several types of morphological changes in the liquid crystalline texture under in situ PLM. Figure 2 displays the photographs of coalescence of LC droplets. The dark areas in the micrographs are the isotropic phase, while the bright areas represent the anisotropic phase. The domain growth and coalescence of LC droplets lead to the formation of schlieren texture. The fraction of the isotropic phase becomes smaller and smaller, while the LC phase grows quickly to the full view range. Highlighted in a black circle in Figure 2 is an obvious coalescence of the LC droplets.

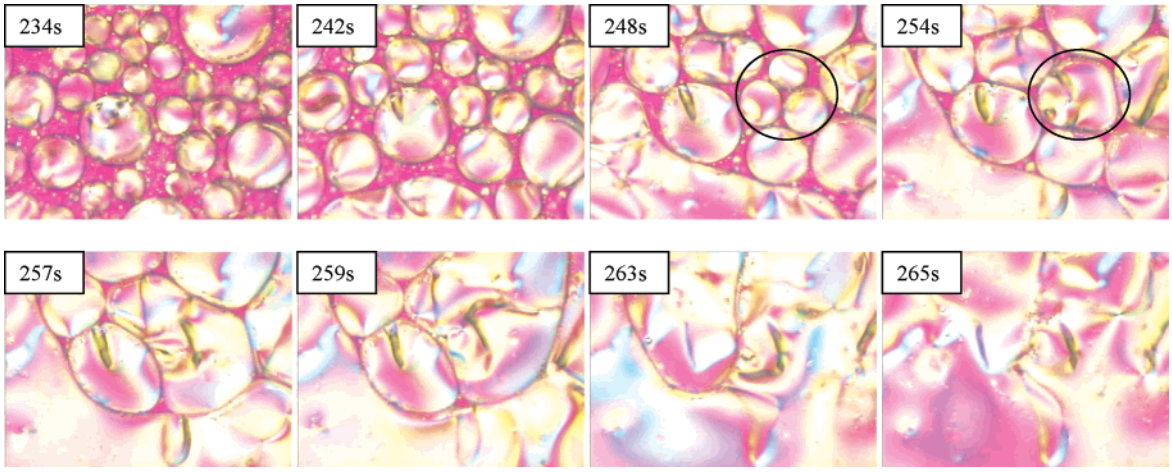

Figure 2. Coalescence of LC domains in 70/15/15 ABA/BP/TDA reaction system. Micrographs were obtained from the same area of the same sample. Reaction temperature: 380 °C.

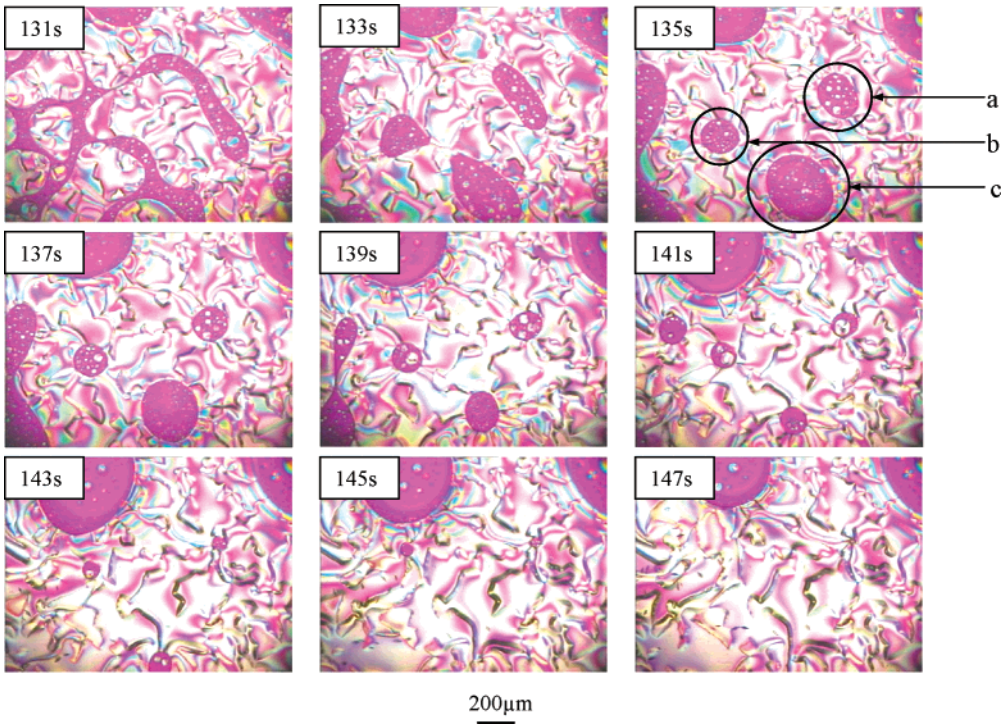

Figure 3. Changes of isotropic areas (**a**, **b**, and **c**) with time. Micrographs were obtained from the same area of the same sample. Reaction system: 70/15/15 ABA/BP/TDA. Reaction temperature: 380 °C.

Figure 3 shows the rapid conversion of isotropic phase to schlieren texture. It took only 20 s from the formation of isotropic round areas to their disappearance. The morphological changes of the isotropic areas (**a**, **b**, and **c**) are illustrated. It can be seen that the isotropic areas become smaller and rounder with the reaction proceeding. The tendency to form round areas is understandable, which minimizes the interface of two phases and consequently lowers the surface energy.

Figure 4 indicates the isotropic area changes as a function of time. Generally, the isotropic round area becomes smaller and its downsize rate decreases with time. The viscosity change and the polymerization kinetics both play critical roles for the decrease of the isotropic areas.

Schlieren textures characterized by dark brushes meeting at a dark point can be observed when the thickness of nematic liquid crystals is thin (about 10−20 μm). If the polarizer and the analyzer are rotated simultaneously, the black brushes move continuously over the field, indicating a continuous change in the direction of the optical axis in the layer. On the other hand, the point from which the brushes start does not change its position during the rotation of the polarizers. According to

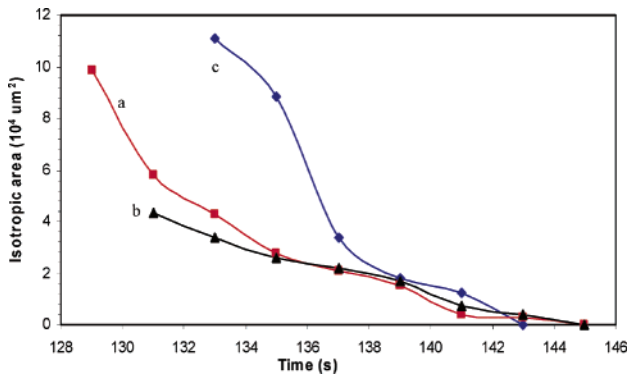

Figure 4. Time dependence of isotropic areas **a**, **b**, and **c** in the LC phase. The specific isotropic areas are labeled in Figure 3. Reaction system: 70/15/15 ABA/BP/TDA. Reaction temperature: 380 °C.

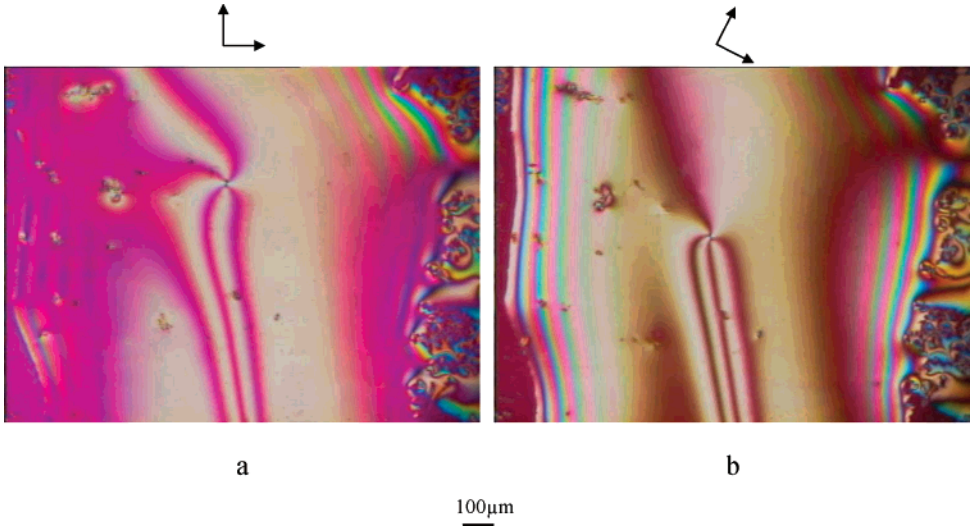

Figure 5. Micrographs showing image change of black brushes when rotating crossed polarizers clockwise for 30 °C from (a) to (b). Micrographs were obtained from the same area of the same sample. Sample: 70/15/15 ANA/AAA/TDA system reacted at 380 °C for 12 min.

Nehring and Saupe,[41] this type of point is caused by line singularities perpendicular to the layer, and the term "point singularity" was suggested for this type of line singularities because of their appearance. They showed that the point singularity can be characterized by $|S| = N/4$ (N is the number of brushes) with a positive or negative sign. A positive sign is given when the brushes rotate in the same direction as that in which the polarizer and analyzer are simultaneously rotated in the crossed position, whereas a negative sign is assigned when they turn in the opposite direction. Figure 5b was obtained after the polarizers were rotated clockwise by 30° relative to the position in the case of Figure 5a. The actual vibration directions for the polarizer and analyzer are shown by the dark cross in the image of a nematic domain. In Figure 5a, the vibration direction of the analyzer is vertical; in Figure 5b it is at the position turned clockwise by 30°. The point singularities in the middle of the figures are thus assigned the S value of $+1$.

On the basis of our PLM experimental results on six aromatic polyester reaction systems, we found all morphological changes (the above phenomena and those mentioned in the following) of LC textures during thin film polymerization are universal (i.e., $S = +1$). Thus we may deduce the morphological changes and the annihilation processes studied in our study are of universality for aromatic LC polyesters.

3.2. General Trend of the Annihilation between Disclinations and Its "Tail" Effect. Disclinations contain excess free energy and tend to reduce in number, resulting in the reduction of free energy and molecular direction. Consequently, the free energy relaxation is accompanied by an increase in domain size with uniform molecular orientation. However, annihilation between the defects is a complicated process and is not fully understood yet. We found that the annihilation process is affected by many factors. For example, other defects surrounding the particular pair of defects more or less affect the annihilation. In addition, the increase in elastic constant due to molecular weight increase during polymerization adds the other complicated factor to the annihilation process. However, that the annihilation rates for different pairs of disclinations decrease with reaction time is a universal trend according to previous studies.[26,37,42−44]

Shiwaku et al.[13] observed the number of disclinations in a thermotropic LCP decreasing with annealing time. They suggested that the structural order evolution with time may be expressed by the square root of the average area per disclination line d (μm) (i.e., the average spacing between two neighboring disclinations) vs annealing time t (s) as the following scaling relation:

$$d \sim t^{0.35} \tag{2}$$

In the mean-field argument,[37] the scaling exponent $\nu = 1$ because the system is considered to consist of isolated pairs of defects at random separation distances and the rate of defect density ρ change is proportional to the probability of binary collisions:

$$\frac{d\rho}{dt} \sim -\rho^2 \tag{3}$$

This value is not usually observed in experiments. In reality, isolated pairs are rare: each defect is surrounded by a host of other defects, some with positive and others with negative sign. Therefore, the path which two defects follow to annihilation may not be a simple straight line drawn between the pair but may be rather tortuous. The process is further complicated by the simultaneous movements of all defects; thus, constant background force changes affect any pair of defects. The effect of such a collective motion is to slow the process, leading to a power law exponent with a magnitude smaller than 1.

Figure 6 shows PLM micrographs of an annihilation process between a pair of defects at different reaction times, while Figure 7a displays the time dependence of the distance d between the disclination pair.

At the beginning of polycondensation, the annihilation occurs very quickly, since the molecular weight at this stage is relatively low and thus viscosity of the system is not very high. With an increase in the reaction time, the annihilation rate slows down because the increasing viscosity restricts the motion of disclinations for further annihilation. When the energy needed for the reorganization of molecular orientation is higher than that released by the annihilation of defects, the annihilation process is completely retarded.

From these two figures, we can see that the annihilation rate ($\nu = dD/dt$; dD is the change in distance between the two defects and dt is the change in time) in the early stage of annihilation remains approximately the same, which follows a power law. The slope in the early stage of the annihilation process is about 1.70.

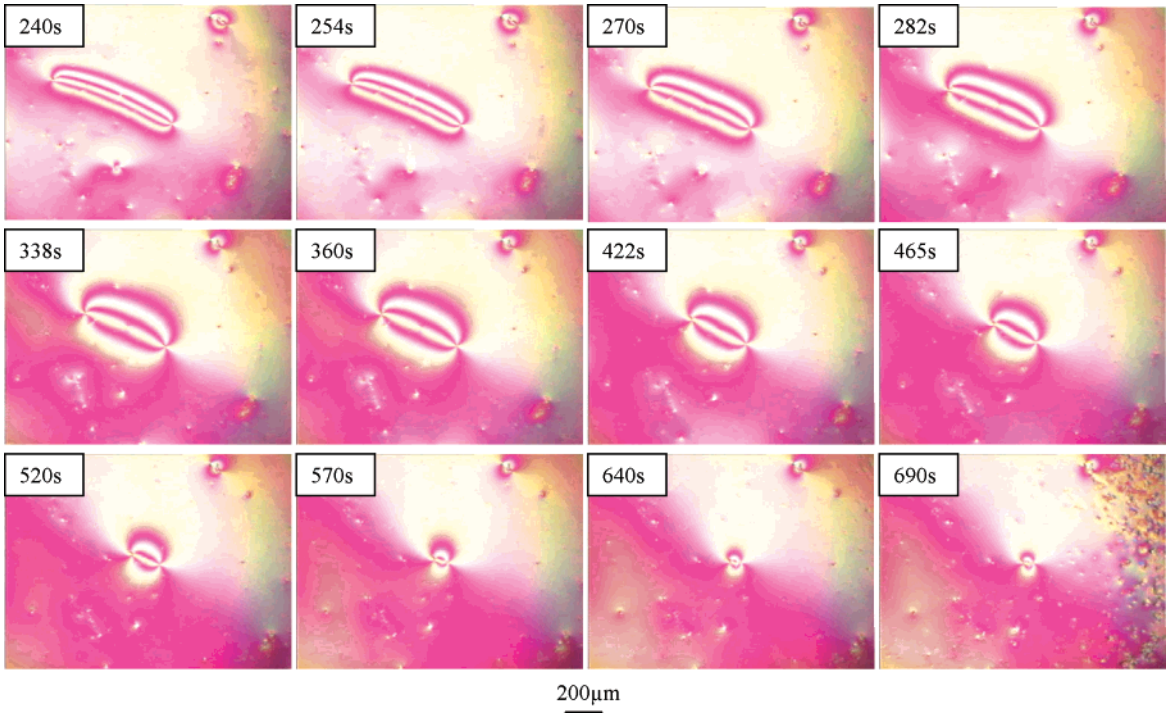

Figure 6. Micrographs showing annihilation process of a disclination pair of the LC system. Micrographs were obtained from the same area of the same sample. Reaction system: 70/15/15 ABA/AAA/TDA. Reaction temperature: 380 °C.

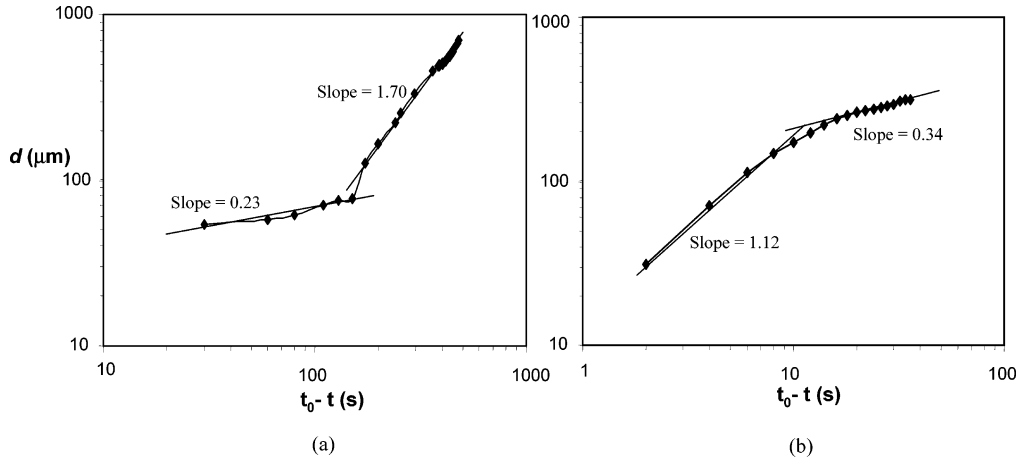

Figure 7. Time dependence of distance *D* between disclination pairs: (a) disclination pairs shown in Figure 6; (b) disclination pairs shown in Figure 8. *t* is reaction time; t_0 is the time that two disclinations joined and disappeared. Reaction system: 70/15/15 ABA/AAA/TDA system. Reaction temperature: 380 °C.

In the late stage, the "tail effect"with a slope of 0.23 appears.[26] The rate decrease is exactly the same as what we predicted in the previous section. Since Figure 6 indicates that the surrounding environments are without any other disclinations, the disclination pair should annihilate freely without being affected by other annihilations. Thus the cause of rate decrease in annihilation is mainly due to the fact that crystallization began to appear in some places in the late stage, at about 640 s, which brought a big retarding factor to the annihilation process of this disclination pair.

However, a different kind "tail effect"can be observed in other disclination pairs in Figure 8 and analyzed in Figure 7b. In the early stage the annihilation rate is 0.34, while the rate in late stage surprisingly increases to 1.12, showing a faster annihilation rate. *This presents a totally different trend from the previous case*. Figure 8 displays the details of evolution of annihilation. The disclination pair appears because of the coalescence of two adjacent LC droplets. Two defects that are in two separate LC droplets connected and a disclination pair forms. The new pair follows the principle of free energy decrease and reduces their distance with time. The cause of different tail effects probably mainly arises from the environmental effects on the disclination pairs.

In Figure 6 there is no other disclination around; thus the disclination pair can annihilate freely without being affected by other annihilations. The lower annihilation rate in the late stage is caused by the occurrence of crystallization in their surroundings. By contrast, in Figure 8 there are other disclinations around the one we are studying. Since all disclinations undergo annihilation courses, they must have either retardation or acceleration effects on one another. Retardation seems to occur more often according to our experimental results. As shown in Figure 8, the number of disclinations in the system studied becomes much less in the late stage. Thus, the two disclinations that we are studying can annihilate freely and more quickly without much influence from their surroundings. The

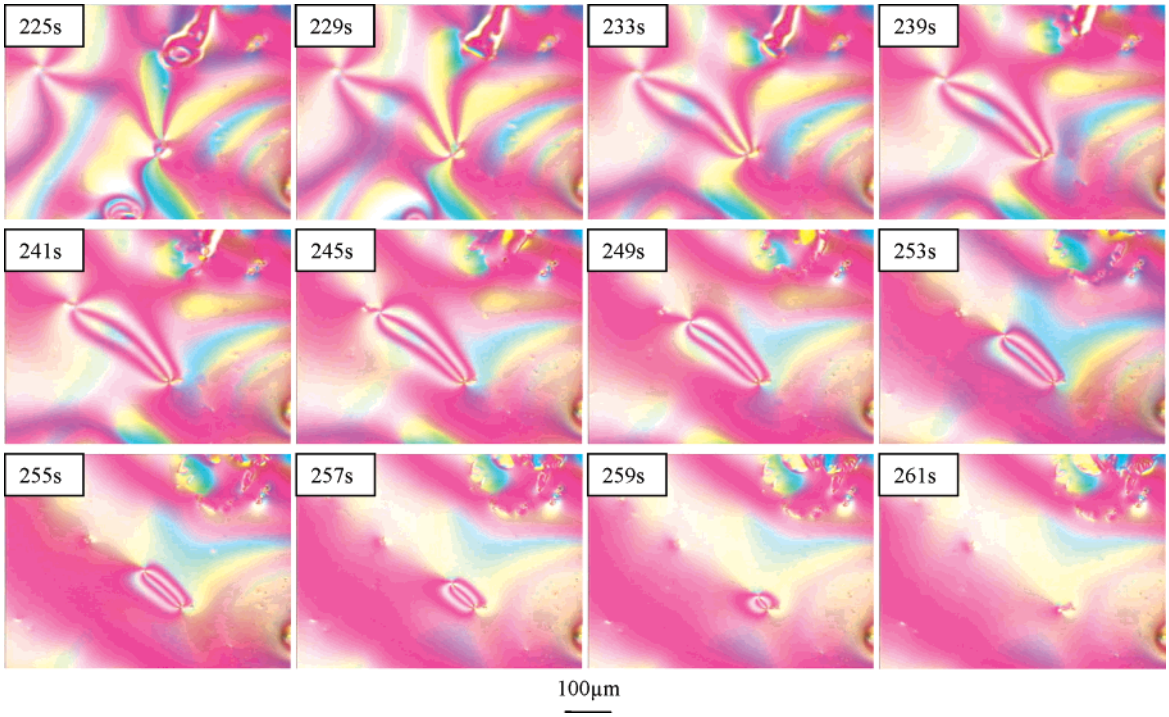

Figure 8. Micrographs of another disclination pair showing different trend of the annihilation rate in LC system annihilation process. Micrographs were obtained from the same area of the same sample. Reaction system: 70/15/15 ABA/AAA/TDA. Reaction temperature: 380 °C.

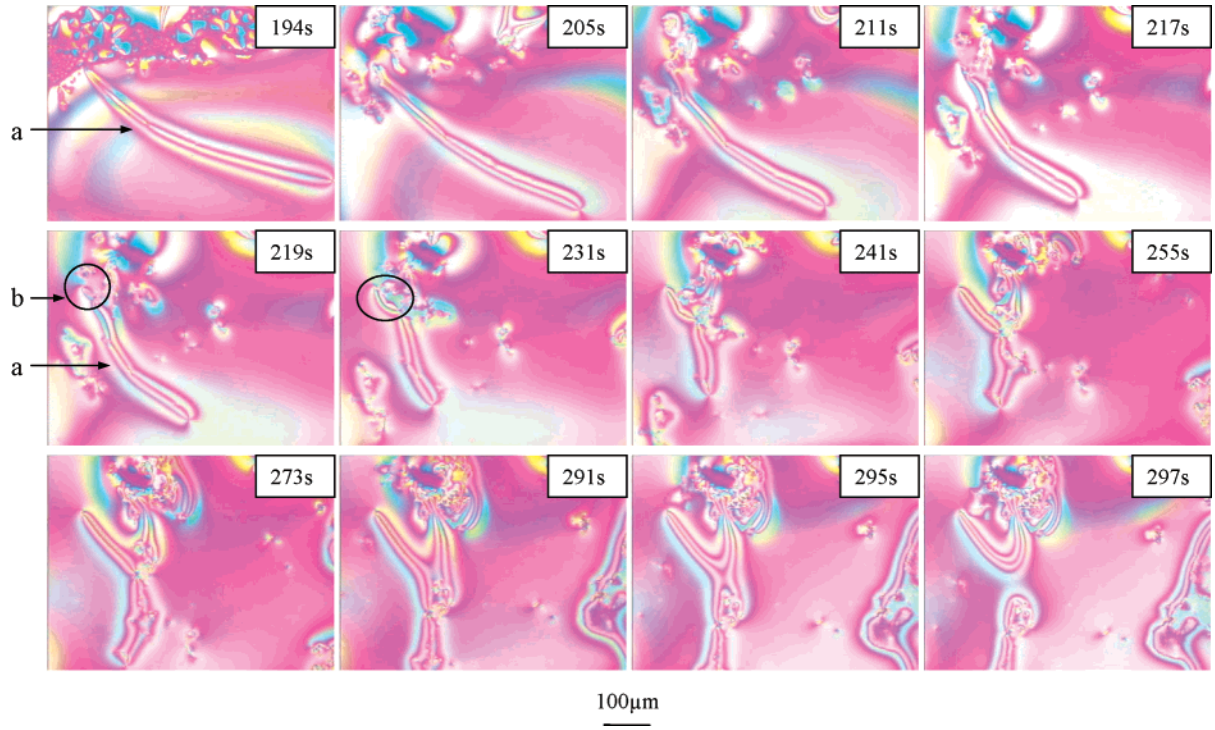

Figure 9. Micrographs showing annihilation process of disclination pairs **a** and **b** in the LC system. Micrographs were obtained from the same area of the same sample. Reaction system: 70/15/15 ABA/DABP/TDA. Reaction temperature: 380 °C.

annihilation rate is about 0.34, which is quite near that from previous literature reports.[13,42]

3.3. Increase in the Distance between Two Disclinations. It is known that disclinations contain excess free energy, so they tend to reduce in number and result in the reduction of net free energy. Therefore, a decrease in the distance of disclination pairs with reaction time is a universal trend. However, in our study we have observed the opposite phenomenon, namely, an increase in pair distance with time. Figure 9 shows two disclination pairs (**a** and **b**) during 174−300 s. Pair **a** exhibits a conventional annihilation process in the early stage from 174 to 243 s. Its distance decreases from 601.7 μm at 194 s to 157.0 μm at 243 s with a rate of about 15.11 μm/s. However, afterward, the annihilation does not continue while the distance of the two disclinations becomes larger. The distance increases from 157.0 μm at 243 s to 193.4 μm at 273 s, although the rate

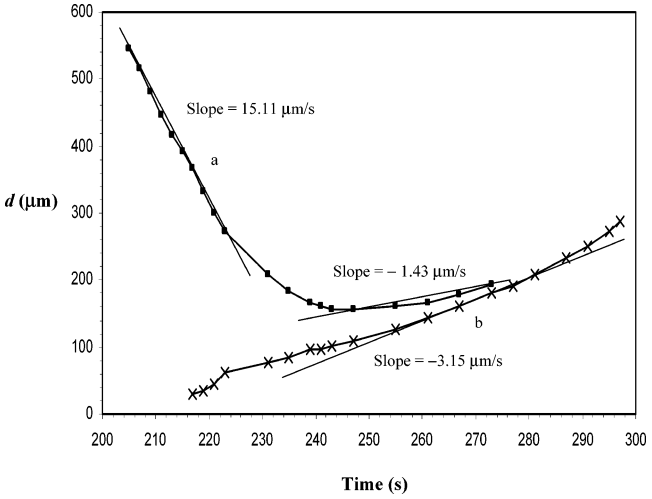

Figure 10. Time dependence of distances *D* between disclination pairs **a** and **b** shown in Figure 9. Reaction system: 70/15/15 ABA/DABP/TDA system. Reaction temperature: 380 °C.

is comparatively much slower (−1.43 μm/s), as shown in Figure 11. Here we define "−" rate for distance increase between the defect pair and "+" rate for distance decrease.

The disclination pair **b** appears at about 217 s. Interestingly the distance for this disinclination pair does not become shorter with time as those for general disclination pairs do. Instead, it grows longer with time. At 217 s, it is about 28.9 μm, while at 297 s it has grown to 287.6 μm. The rate calculated from Figure 10 is about −3.15 μm/s.

To our best knowledge, this interesting phenomenon has not been reported before. Two reasons may be accounted for this phenomenon. First, this system is a reaction system, which is undergoing chain growth in the early stage. The trend of annihilation of the disclination pair may be surpassed by the trend of chain growth. Thus the disclination pair distance cannot get shorter but increases during the annihilation. The other possible reason is due to the effect of the surroundings. Figure 10 clearly shows that there are many disclinations around the disclination pair **b** and they exert much effect on one another's annihilations.

3.4. Formation of the Disclination Pairs. Generally a disclination pair is formed during the coalescence process of two adjacent LC droplets. When two LC droplets make contact, they have the tendency to become one domain to reduce the free energy; so do the LCPs studied in the current system. Figure 11a displays an example.

The other situation to form a disclination pair is shown in Figure 11b. It originates from the reorganization of disclinations. In other words, a LC system has the tendency to reduce its overall free energy of the entire system. When the LC phase appears, especially in a reaction system to form liquid crystallinity, it usually evolves many disclinations rapidly in the initial stage. Many disclinations simultaneously evolve, annihilate, and reorganize rapidly to form a more stable state with fewer disclinations. Figure 11b is a typical example. At 119 s, many defects can be observed in the system. Two seconds later, these disclinations reorder and a new disclination pair is therefore formed, which is indicated by the arrow. This new disclination pair then follows the general rule to annihilation.

Similar to the LC system, we also observed the combination of two disclination pairs to one disclination pair. As illustrated in Figure 11c, two disclination pairs approach to each other at 229 s and then combine to form one disclination in 2 s. The new one recombines with another disclination pair (not shown in this Figure) in 4 s more.

3.5. FTIR Characterization and Inherent Viscosity Measurements. Parts a and b of Figure 12 display the FTIR spectra of the monomers and thin film products of the 70/15/15 ABA/AAA/TDA reaction system. The occurrence of polycondensation and transesterification among the monomers during thin film polymerization is confirmed by FTIR spectra. The detailed

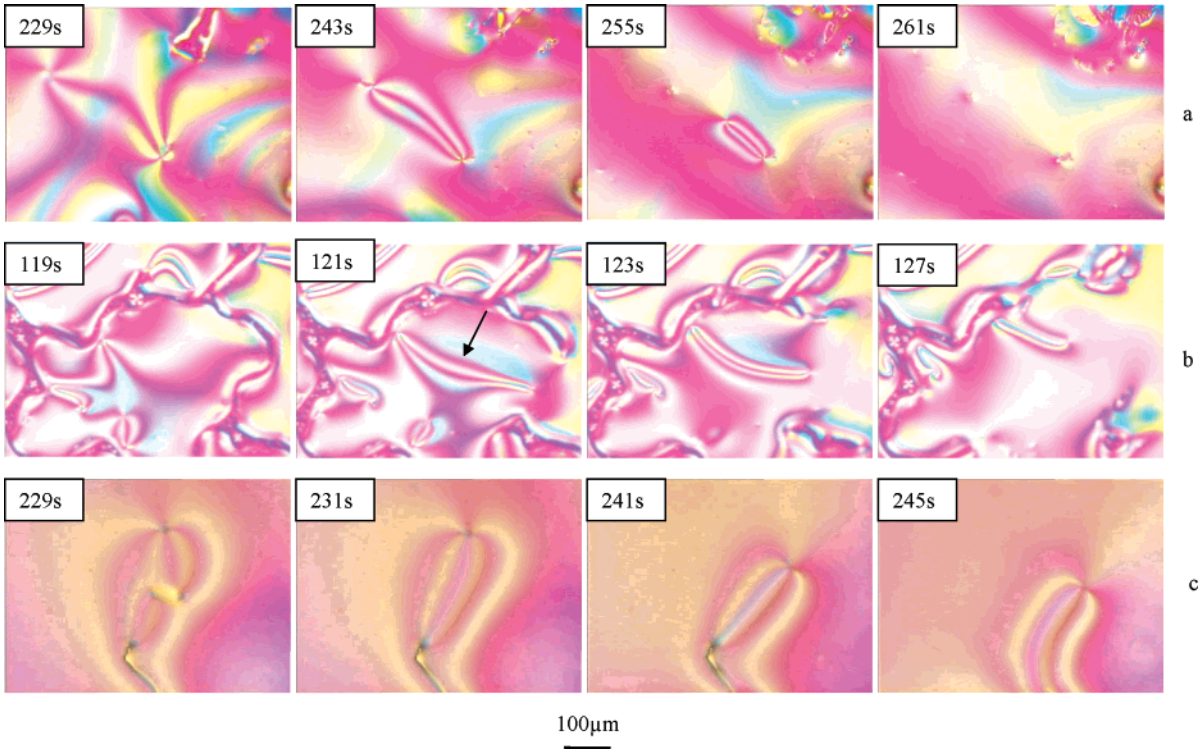

Figure 11. Micrographs showing formation of disclination pairs in the LC system. Micrographs were obtained from the same area of each sample. Reaction system: (a) 70/15/15 ABA/AAA/TDA, (b) 70/15/15 ABA/DABP/TDA, and (c) 70/15/15 ANA/BP/TDA. Reaction temperature: 380 °C.

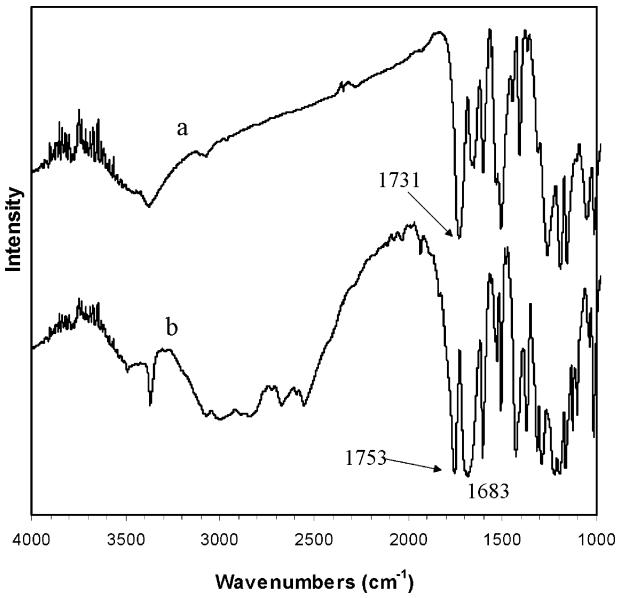

Figure 12. FTIR spectra of monomer mixture and thin film polymerization products for the 70/15/15 ABA/AAA/TDA system: (a) before reaction (monomer mixtures) and (b) after 1 h thin film polymerization at reaction temperature of 380 °C.

analysis of FTIR spectra has been published elsewhere.[45] In summary, the FTIR spectra suggest that the OH group from carboxylic acid and the acetyl groups from acetate and acetamide have disappeared and the copolymer has been synthesized after 1 h of reaction. The existence of TDA is confirmed by the out-of-plane bending of the $C_\beta-H$ of 2,5-disubstituted thiophene ring at 736 cm^{-1}. These observations confirm the occurrence of esterification and polycondensation among the three monomers and hence the formation of a substantial amount of ester and amide groups.

The inherent viscosity (IV) values of the thin film polymerized Vectra 72/27 ABA/ANA and 70/15/15 ABA/AAA/TDA systems were tested. The value for the 72/27 ABA/ANA system was about 2.7, which was regarded as acceptable because the IV range for that LCP should be 2.6−6.5 as mentioned in a US patent.[46] However, our LCP products did not dissolve in any common solvents or in those commonly used for LCPs, such as 3,5-bis(trifluoromethyl)phenol (BTMP) and pentafluorophenol (PFP). Thus, we were unable to do GPC or light scattering measurements due to the insolubility of the polymers.

4. Conclusion

Several aromatic liquid crystalline polyester reaction systems were employed to study the annihilation of defects and disclinations. Generally, the decrease of the isotropic areas in the LC phase and the annihilations between two defects are observed to obey the power law. However, in contradiction to conventional rules, we also observed a faster annihilation rate in the late stage of the annihilation process in some samples and an increase in the distance of a disclination pair in our experiments because of the surroundings and polymerization effects. The formation of the disclination pairs results from the coalescence process of two adjacent LC droplets, rearrangement of disclinations, and the combination of two disclination pairs.

Acknowledgment. Financial support from the National University of Singapore (NUS) under Research Grant RP 279-000-105-112 is gratefully acknowledged. Special thanks are given to Sumitomo Chemical (Japan) for their valuable free samples and information, Ueno Fine Chemicals (Japan) and Teijin (Japan) for provision of free HBA and HNA monomers.

References and Notes

(1) Mazenko, G. F.; Zannetti, M. *Phys. Rev. B* **1985**, *32*, 4565.
(2) Pasquale, F. de; Tartaglia, P. *Phys. Rev. B* **1986**, *33*, 2081.
(3) Toyoki, H.; Honda, K. *Prog. Theor. Phys.* **1987**, *78*, 237.
(4) Bray, A. J. *Phys. Rev. Lett.* **1989**, *62*, 2841.
(5) Nishimori, H.; Nukii, T. *J. Phys. Soc. Jpn.* **1988**, *58*, 563.
(6) Mondello, M.; Goldenfeld, N. *Phys. Rev. A* **1990**, *42*, 5865.
(7) Chung, I.; Yurke, B.; Pargellis, A. N. *Phys. Rev. E* **1993**, *47*, 3343.
(8) Yurke, B.; Pargellis, A. N.; Chung, I. *Physica B (Amsterdam)* **1992**, *178B*, 56.
(9) Chung, I.; Turok, N.; Yurke, B. *Phys. Rev. Lett.* **1991**, *66*, 2472.
(10) Chung, I.; Durrer, R.; Turok, N.; Yurke, B. *Science* **1991**, *251*, 1336.
(11) Orihara, H.; Ishibiashi, Y. *J. Phys. Soc. Jpn.* **1986**, *55*, 2151.
(12) Nagaya, T.; Orihara, H.; Ishibiashi, Y. *J. Phys. Soc. Jpn.* **1987**, *56*, 3086.
(13) Shiwaku, T.; Nakai, A.; Hasegawa, H.; Hashimoto, T. *Polym. Commun.* **1987**, *28*, 174; *Macromolecules* **1990**, *23*, 1590.
(14) Thomas, E. L.; Wood, B. A. *Faraday Discuss. Chem. Soc.* **1985**, *79*, 229.
(15) Chen, S.; Du, C.; Jin, Y.; Qian, R.; Zhou, Q. *Mol. Cryst. Liq. Cryst.* **1990**, *188*, 197.
(16) Wang, W.; Lieser, G.; Wegner, G. *Liq. Cryst.* **1993**, *15*, 1.
(17) Hudson, S. D.; Fleming, J. W.; Gholz, E.; Thomas, E. L. *Macromolecules* **1993**, *26*, 1270.
(18) De'Nève, T.; Navard, P.; Kléman, M. *Macromolecules* **1995**, *28*, 1541.
(19) Ernst, B.; Navard, P.; Hashimoto, T.; Takebe, T. *Macromolecules* **1990**, *23*, 1370.
(20) Takebe, T.; Hashimoto, T.; Ernst, B.; Navard, P.; Stein, R. S. *J. Chem. Phys.* **1990**, *92*, 1386.
(21) Picken, S. J.; Aerts, J.; Doppert, H. L.; Reuvers, A. J.; Northolt, M. G. *Macromolecules* **1991**, *24*, 1366.
(22) Picken, S. J.; Moddenaers, P.; Berghmans, S.; Mewis, J. *Macromolecules* **1992**, *25*, 4759.
(23) Pargellis, A. N.; Turok, N.; Yurke, B. *Phys. Rev. Lett.* **1991**, *67*, 1570.
(24) Nagaya, T.; Hotta, H.; Orihara, H.; Ishibiashi, Y. *J. Phys. Soc. Jpn.* **1991**, *60*, 1572; *J. Phys. Soc. Jpn.* **1992**, *61*, 3511.
(25) Mason, N.; Pargellis, A. N.; Yurke, B. *Phys. Rev. Lett.* **1993**, *70*, 190.
(26) Ding, D.-K.; Thomas, E. L. *Mol. Cryst. Liq. Cryst.* **1994**, *241*, 103.
(27) Toussaint, D.; Wilczek, F. *J. Chem. Soc., Faraday Trans.* **1995**, *91*, 2497.
(28) Toyoki, H. *Phys. Rev. B* **1992**, *45*, 1965.
(29) Bray, A. J. *Physica A* **1993**, *194*, 41.
(30) Liu, F.; Mazenko, G. F. *Phys. Rev. B* **1993**, *47*, 2366.
(31) Orihara, H.; Ishibiashi, Y. *J. Phys. Soc. Jpn.* **1992**, *61*, 1.
(32) Yurke, B.; Pargellis, A. N.; Kovacs, T.; Huse, D. A. *Phys. Rev. E* **1993**, *47*, 1525.
(33) Toyoki, H. *J. Phys. Soc. Jpn.* **1994**, *63*, 4446.
(34) Windle, A. H.; Assender, H. E.; Levine, M. S. *Proc. R. Soc. London, Ser. A* **1994**, *348*, 73.
(35) Jang, W. G.; Ginzburg, V. V.; Munzy, C. D.; Clark, N. A. *Phys. Rev. E* **1995**, *51*, 411.
(36) Pargellis, A. N.; Finn, P.; Panizza, P.; Yurke, B.; Cladis, P. E. *Phys. Rev. A* **1992**, *46*, 7756.
(37) Liu, C.; Muthukumar, M. *J. Chem. Phys.* **1997**, *106*, 7822.
(38) Cheng, S. X.; Chung, T. S.; Mullick, S. *Chem. Eng. Sci.* **1999**, *54*, 663.
(39) Cheng, S. X.; Chung, T. S.; Mullick, S. *J. Polym. Sci., Part B: Polym. Phys.* **1999**, *37*, 3084.
(40) Asrar, J.; Toriumi, H.; Watanabe, J.; Krigbaum, W. R.; Ciferri, A. *J. Polym. Sci., Part B: Polym. Phys. Ed.* **1983**, *21*, 1119.
(41) Nehring, J.; Saupe, A. *J. Chem. Soc., Faraday Trans. 2* **1972**, *68*, 1.
(42) Shiwaku, T.; Nakai, A.; Wang, W.; Hasegawa, H.; Hashimota, T. *Liq. Cryst.* **1995**, *19*, 679.
(43) Wang, W.; Hashimota, T. *Liq. Cryst.* **1996**, *20*, 669.
(44) Wang, W.; Shiwaku, T.; Hashimota, T. *J. Chem. Phys.* **1998**, *108*, 1618.
(45) Xu, J. M.; Wang, Y.; Chung, T. S.; Goh, S. H. *J. Mater. Res.* **2003**, *18*, 1509.
(46) Calundann, G. W. U.S. Patent 4,067,852, 1978; U.S. Patent 4,161,470, 1979; U.S. Patent 4,184,996, 1980. East, A. J.; Charbonneau, L. F.; Calundann, G. W. U.S. Patent 4,330,457, 1982 (to Hoechst Celanese).